JOURNAL OF MATERIALS SCIENCE **34** (1999) 6143–6149

Phase transitions due to polar region structure in disordered ferroelectrics

HUIQING FAN*
State Key Laboratory of Solidification Processing, Northwestern Polytechnical University, Xi'an 710072, People's Republic of China
E-mail: hqfan@ihw.com.cn

LINGBING KONG, LIANGYING ZHANG, XI YAO
Electronic Materials Research Laboratory, Xi'an Jiaotong University, Xi'an 710049, People's Republic of China

We show clear experimental evidence for two phase transitions in titanium doped lead magnesium niobate compositional disordered ferroelectrics. One is the diffuse phase transition near the temperature of the dielectric permittivity maximum, which is often called the characteristic of relaxor ferroelectrics (relaxors). Another is a first-order transformation from relaxor ferroelectric to normal ferroelectric, corresponding to a zero-field spontaneous polar micro-macrodomain switching. According to X-ray diffraction (XRD) measurements, thermal analysis and transmission electron microscope (TEM) results, a dynamic behavior of polar microregions is necessary to explain the phenomena, which is more similar to a stress induced martensitic transformations form cubically stabilized perovskite parent-phase. It is also observed that the dynamic behavior of polar regions was influenced by the titanium doping.

1. Introduction

During the past several decades years, much attention has been focused on understanding the relaxational properties and phase transitions in strongly compositional disordered ferroelectrics, such as $Pb(Mg_{1/3}Nb_{2/3})O_3$ (PMN), $Pb(Sc_{1/2}Ta_{1/2})O_3$ and La modified $PbZr_{1-x}Ti_xO_3$ (PLZT) [1–4]. However, up to now, the nature and the mechanisms of the phase transitions and relaxation are not clearly understood.

For the present study we selected titanium doped lead magnesium niobate compositional disordered ferroelectrics. The substitution of titanium on the B sites in lead magnesium niobate leads to a well-known family of ceramics having the chemical formula $Pb(Mg_{1/3}Nb_{2/3})_{1-x}Ti_xO_3$, or PMNT, with unusual dielectric and piezoelectric properties [5, 6]. The Mg^{2+} and Nb^{5+} ions, which are randomly distributed on the B sites, represent a type of disorder which significantly modifies the properties of these materials. One manifestation of this disorder is the condensation of local dipolar nanodomains leading to local, randomly oriented polarization at a temperature much higher than the ferroelectric transition temperature (T_c). These polar nanodomains increase in size with decreasing temperature and for relatively high titanium concentration, ultimately result in the formation of macroscopic ferroelectric domains with long-range ferroelectric order. The peak in the dielectric permittivity at T_c is relatively sharp and independent of frequency below the GHz range (radio frequency range). For a low titanium concentration, the disorder hinders the onset of long-range order, and the polar nanodomains condense below the freezing temperature (T_m) of the polarization fluctuations into glasslike, or relaxor, state with no macroscopic phase (symmetry) change.

For the particular composition of 20% Ti doped $Pb(Mg_{1/3}Nb_{2/3})O_3$, the relaxor behavior and phase transition are very interesting. In the present paper, we studied the phase transitions in $Pb(Mg_{1/3}Nb_{2/3})_{0.8}Ti_{0.2}O_3$ ceramics using the dielectric, polarization, thermal, and X-ray diffraction measurements. A new phase transition is clearly observed, which is called a spontaneous, first-order relaxor to normal ferroelectric transition on cooling in the absence of a poling electric field. Specifically, this transition has been observed in disordered PST, PLZT 12/40/60 and other relaxor systems [7–9]. But, the physical mechanisms of relaxor-normal ferroelectric transition is not well understood. Thus, the aim of this study was to find a clear understanding of all the phase transitions. Additionally, the compositional effect of titanium doping is discussed briefly.

2. Experimental

For the preparation of $Pb(Mg_{1/3}Nb_{2/3})_{1-x}Ti_xO_3$ ($x = 0.0, 0.1, 0.2, 0.4$; designated as PMNT1-x/x) ceramic samples a two-step method was used [10]. Starting chemical materials were PbO, MgO, Nb_2O_5, and

* Author to whom all correspondence should be addressed.

TiO_2 (99.9% purity). Samples for electrical measurements were electroded with low temperature-fired silver paint.

The weak-field dielectric response was measured by using a Hewlett Packard 4274A LCR meter which can cover a frequency range from 100 Hz to 100 kHz. Samples were placed in a test chamber, which can be operated between −196 °C and 250 °C. The amplitude level of the signal was 5 V/cm. The thermal depoling current was measured as a function of temperature with HP 4140B PA meter. The spontaneous polarization can be calculated by back integration [11]. The ferroelectric hysteresis loop (P-E) were characterized by using a computer-controlled, modified Sawyer-Tower circuit. 1 Hz sine wave voltages were applied to the samples by a Trek 610 high voltage amplifier for which input signals were generated by the computer. Output signals from the samples were get and processed by the computer.

Differential scanning calorimetry (DSC) measurements were carried out on a TA2100 automatic thermal analysis system. Small block and powder samples of ceramics were separately used as specimens in this analysis. Thermal expansion measurements were also taken by a TA 2100 dilatometer between 20 and 500 °C (accuracy ca 20 nm). The rods of the sample to be studied were placed between two polished, fused quartz plates. In this cases the rods were about 5 mm long by 1 mm thick.

In order to examine the domain structure, Thin foils were prepared by standard ceramographic techniques using a Gatan 'dual-ion mill' (model 600) operated at 5kV with a combined gun current of 1 mA. The foils were investigated using a JEOL JEM-200 CX transmission electron microscope.

A Rigaku DMAX-3 X-ray diffractometer was used to analysis the phase structure of the samples employing CuK_α radiation. A heating element was placed below the sample and the surface temperature of the sample was measured in a separate temperature cycle without changing the sample condition. Ceramic pellets with ground and polished surfaces were studied.

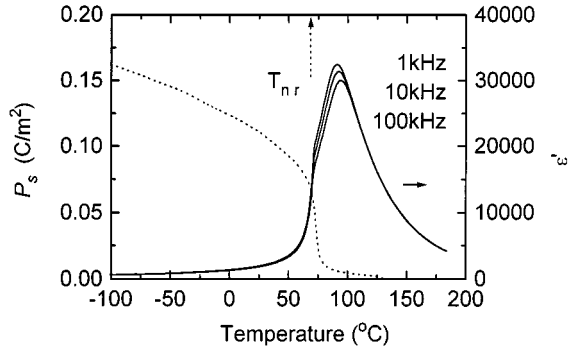

Figure 1 Temperature dependence of the dielectric permittivity at 1, 10, and 100 kHz frequencies and the spontaneous polarization for PMNT80/20 sample upon heating measurements.

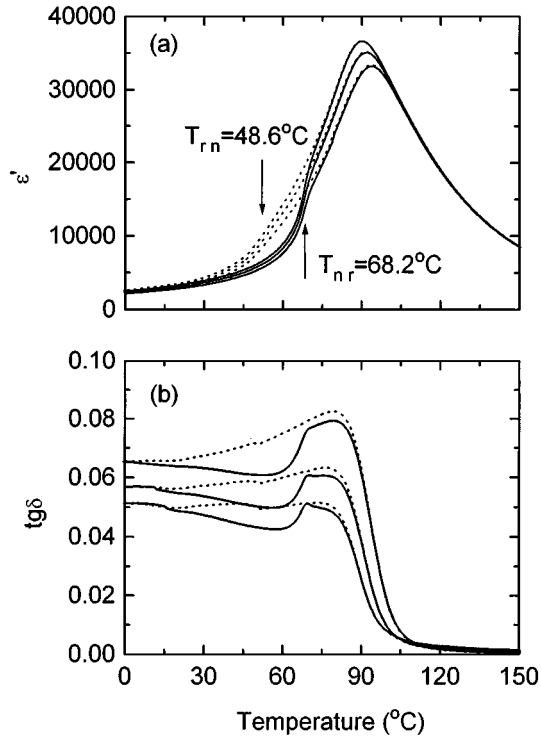

Figure 2 Temperature dependence of (a) the dielectric permittivity and (b) loss angle tangent for PMNT80/20 sample on (. . .) cooling and (—) heating measurements. The frequencies used were 1, 10, and 100 kHz.

3. Results and discussion

3.1. Spontaneous relaxor-ferroelectric transition of $Pb(Mg_{1/3}Nb_{2/3})_{0.8}Ti_{0.2}O_3$

3.1.1. Electrical properties

Fig. 1 shows the real part of dielectric permittivity and the spontaneous polarization as a function of temperature (heating) for $Pb(Mg_{1/3}Nb_{2/3})_{0.8}Ti_{0.2}O_3$ ceramics. A strong frequency dispersion and a shift of the permittivity maximum exist near the temperature of the dielectric permittivity maxima (T_m), which are often called the characteristics of relaxor ferroelectrics (relaxors). Otherwise, the most interesting anomaly is observed at about 68.2 °C. The permittivity increased dramatically near this characteristic temperature, indicated in Fig. 1 as T_{nr}. The spontaneous polarization decreased sharply and then slowly down to zero. It implies a spontaneous transition from normal ferroelectric to relaxor ferroelectric behavior. While during the cooling process, an opposite process was observed near a characteristic temperature, which was marked as T_{rn} in the Fig. 2. It also designates a zero-field spontaneous transformation from relaxor ferroelectric to normal ferroelectric. Relaxor behavior was observed in the temperature region above T_{rn}. These dielectric behaviors are similar to those observed in other relaxor ferroelectrics without any thermal hysteresis near the peak temperature range. However, significant thermal hysteresis effects are evident in the dielectric response around the permittivity anomaly temperature. The difference between T_{rn} and T_{nr} was approximately 19.6 °C. The thermal hysteresis effect suggests the characteristics of a strongly first order phase transformation.

Fig. 3(a–f) shows a sequence of polarization electric field (P-E) hysteresis behaviors for the PMNT80/20 sample for various temperatures respectively. The nonlinear "slim" hysteresis loop can be seen at 156°C, which is characteristic of the absence of a long-range

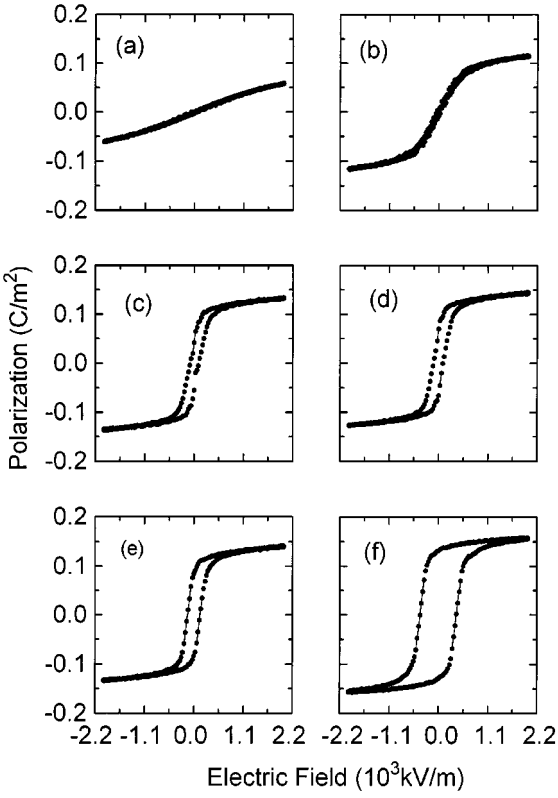

Figure 3 The polarization hysteresis loop P-E for PMNT80/20 sample at temperature of (a) 156 °C, (b) 103 °C, (c) 73 °C, (d) 71 °C, (e) 68 °C, and (f) 15 °C.

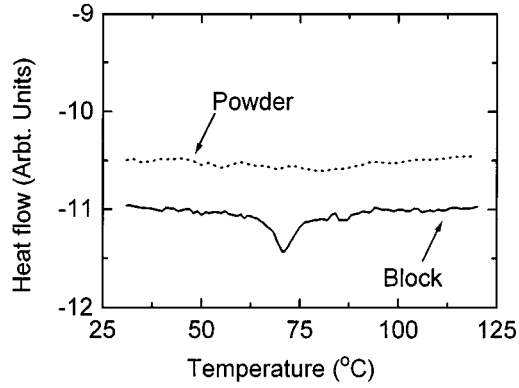

Figure 4 Heat flow as a function of temperature for PMNT80/20 samples in heating measurements.

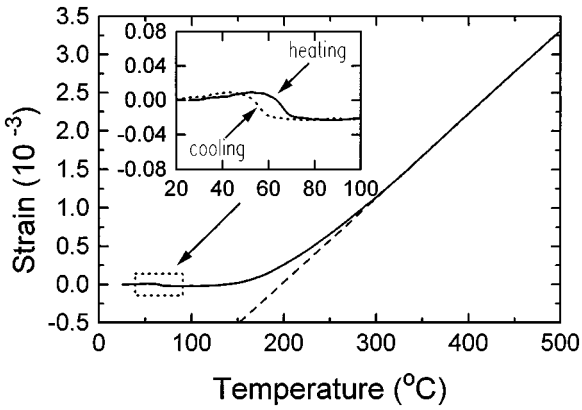

Figure 5 Thermal-expansion strain as a function of temperature for PMNT80/20 sample.

ferroelectric macrodomain and typical of a relaxor ferroelectrics. This temperature is significantly higher than that of T_m(∼105 °C), indicating the presence of local polarization at temperature for above T_m. With decreasing temperature to 103 °C, an enhancement in the saturation polarization was observed, indicating an increase in the volume fraction of local polar regions. As the temperature was further lowered to 73 °C, double loop like feature became evident in the P-E curves, indicating a field induced relaxor-normal transformation. A double loop character was also observed at 71 °C, however the magnitude of the remanent polarization was increased. On cooling to 68 °C, a normal ferroelectric type hysteresis loop became apparent in the polarization behavior. A "square" hysteresis loop is exhibited at 20 °C, which is typical of a phase that contains long-range cooperation between dipoles and which is thus in a ferroelectric macrodomain state. Thus, the first-order normal-relaxor ferroelectrics transition corresponds to a zero-field spontaneous polar micro-macrodomain switching.

It was noted that the dielectric loss angle tangent shows a strong peak, of which the temperature coincides with the temperature of relaxor-normal ferroelectric transitions. It contributed to the internal strain of the ferroelectric micro-macrodomain transition and hysteretic nature of domainwall (DW) motion [12, 13].

3.1.2. Thermal analysis

The discontinuity of permittivity dependence on temperature in PMNT80/20 is due to a phase transition from a normal to relaxor ferroelectric phase, corresponding to a zero-field spontaneous polar micro-macrodomain switching. Several thermal analysis experiments have been carried out in order to provide more information about the nature of this ferroelectric domain switching.

Fig. 4 is a DSC plot of PMNT80/20 powder and block sample. For the block sample, a strong anomaly was shown at 68.0 °C upon heating which is a characteristic of the onset of a phase transition. This anomaly is consistent with the sharp change of permittivity at 68.2 °C on heating, which is shown in Fig. 1. Thus, it can be concluded that this sharp change of permittivity is due to a spontaneous phase transition. Furthermore, absence of the anomaly for the powder sample in DSC response confirms that this phase transition is connected with the internal strain of the ferroelectric micro-macrodomain switching and a discontinuous change of the polar region volume fraction.

Fig. 5 shows the longitudinal strain dependence on temperature upon heating and cooling measurements. Thermal-expansion strain follows a straight line at high temperature. Deviation can be seen from about 350 °C, at which Burns and Dacol suggested that few unit cells become locally polarized [14, 15]. These results are the same as that of other relaxor ferroelectrics [16]. However, inner figure in Fig. 5 gives the anomalies at 68 °C and the strong thermal hysteresis. The thermal-expansion strain follows another straight line at low temperatures. Considering the similarity and difference

between the thermal-expansion strain of PMNT80/20 with that of other relaxor ferroelectrics, we suggest that in PMNT ferroelectric system the Ti doping effect is an increase of the size of the polar microdomains due to the high polarizability of the TiO_6 octahedral which are more effective in overcoming the clustering effect in the 1-1 ordered regions. The size of the latter decreases as well as the random fields originated by them, allowing also the polar domain growth. Until at a transition temperature T_m, polar microdomains transform to polar macrodomains spontaneously, in effect, the structure of the solution changes from distortion cubic to rhombohedral phase.

3.1.3. Phase transition

The X-ray diffraction patterns of pellet PMNT80/20 sample were taken at various temperatures. Fig. 6a and b show the phase transition with temperature for PMNT80/20 sample under cooling and heating measurements. For PMNT80/20 sample with a rhombohedral structure at room temperature, two successive structural phase transitions, cubic-distortion cubic-rhombohedral, take place during cooling and heating. The first transition is gradual and corresponds to the diffused phase transformation from paraelectric to relaxor ferroelectric phase. The second transition is a first-order phase transition, which corresponds to the relaxor-normal ferroelectrics transition. The phase transition character is consistent with its dielectric response and thermal analysis results.

During cooling, PMNT80/20 sample exhibited a continual increase in the degree of X-ray line broadening. This broadening suggests the development of nonuniform strains associated with the rhombohedrality of the polar nanodomains. The local rhombohedral_distortions are small and have a random axial arrangement with respect to each other along equivalent crystallographic direction, yielding an average cubic symmetry. The volume fraction of the polar nanodomains increases with decreasing of temperature, resulting in an increase of the internal strain energy which scales to the volume of the inclusion. The line splitting in (2 0 0) and (2 1 1) reflections suggest the distortion cubic-rhombohedral transition is a first-order phase transformation, and has a thermal hysteresis character. Consequently, on cooling from the polar microdomain state, the thermodynamic stability of system will be decreased relative to that on heating from the long range ferroelectric state. As a result, the thermal hysteresis of the micro-macrodomain switching of relaxor ferroelectrics can be observed.

3.1.4. Transmission electron microscope observations

Fig. 7a and b are bright-field and dark-field TEM images for PMNT80/20 showing tweed striations-like domains. Polar regions developed to a regular ⟨111⟩ ferroelectric macrodomains in this material at room temperature.

The structure is additionally disturbed as in disordered solid solutions or mixed compounds. For a suitable titanium doping in lead magnesium niobate compositional disordered ferroelectrics, a spontaneous transformation from a disordering phase to a phase with lower symmetry with perfect long-range order occurrs. Relaxor state corresponds to a cubical parent phase and nucleating rhombohedral ferroelectric microregion coexistence range. After the spontaneous relaxor-normal ferroelectrics transition, the lower temperature symmetry is sure to be a long-range rhombohedral ferroelectric phase.

3.1.5. Dynamic behavior of polar region

All above results and discussions indicate that the dynamic behavior of polar region is the key to understanding the relaxation properties and phase transition of compositional disordered ferroelectrics [17, 18]. The B site ions in the oxygen octahedron of $A(B'_{1/3}B''_{2/3})O_3$ type perovskite ferroelectrics are shifted from the center along a ⟨111⟩ direction at temperature far above T_m, thus the molecular dipoles are formed. If the lifetime of any of the eight dipole orientations becomes longer than characteristic lattice vibration times, the

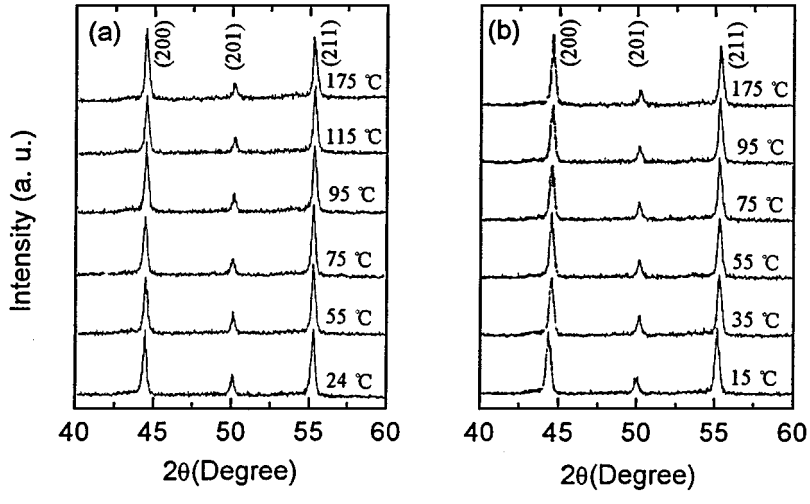

Figure 6 X-ray diffraction patterns of PMNT80/20 sample under (a) heating, and (b) cooling measurements.

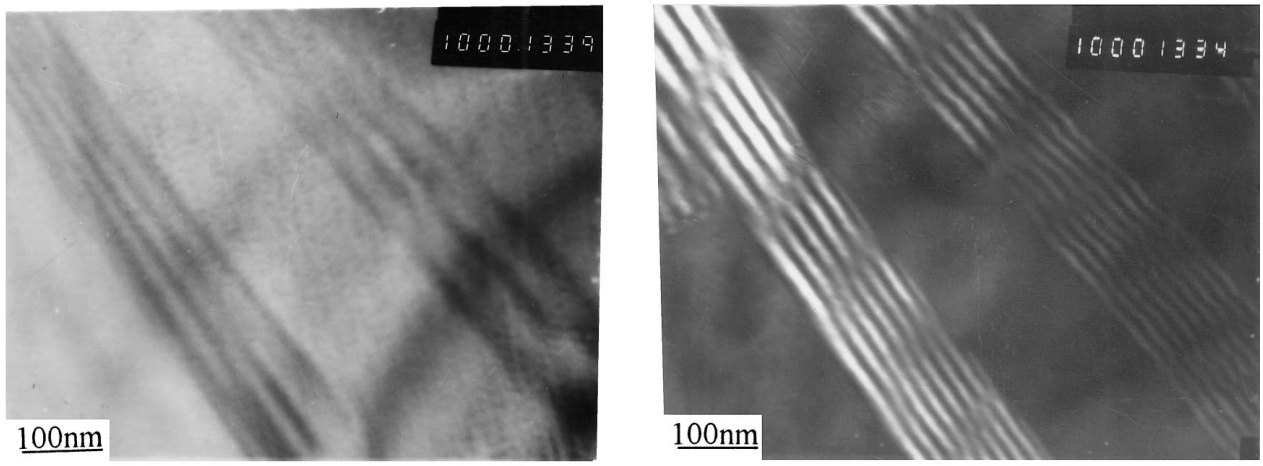

Figure 7 Bright-field (a) and dark-field (b) TEM images which shown tweed striations-like domain structure for PMNT80/20 sample.

positions of the neighboring cations and dipoles will be strongly affected. This cooperative interaction causes the formation of rhombohedral polar regions in the adjacent unit cell. A displacive nucleating phase transition occurred and it is assumed to be the cause of precursor effects in a wide temperature range in the paraelectric phase. The material transformed into relaxor state. The polar vector of local polar regions are thermally hopping among the eight dipole orientations. Down to T_m, the polar vector of polar region gradually froze along one of the eight dipole orientations, thus ferroelectric microdomain forms and the dielectric permittivity shows frequency dispersion. If the electric and elastic interaction of disordered short-range rhombohedral regions is strong enough, a lower symmetry with perfect long-range rhombohedral phase can be spontaneously transformed. A spontaneous relaxor-normal ferroelectric transition occurs, which is similar to a stress induced martensite phase transformation. A crossover from displacive to disorder-order behavior can be clearly seen in rhombohedral PMNT80/20 sample.

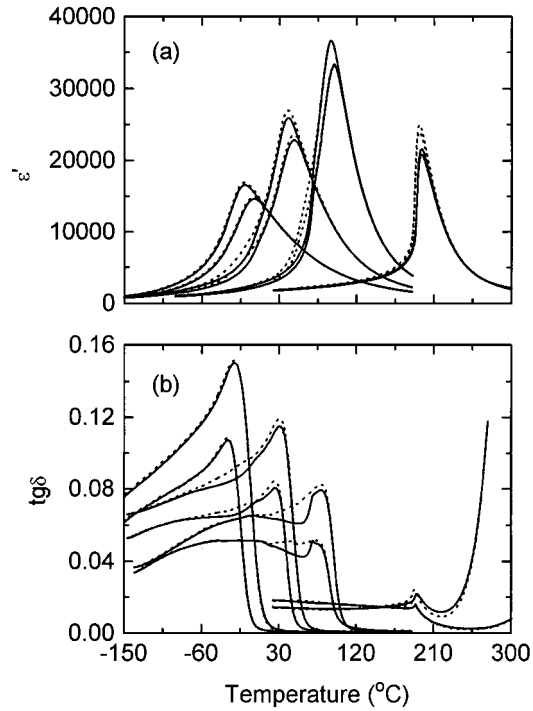

Figure 8 Temperature dependence of the dielectric permittivity (a), and loss angle tangent (b) for PMNT100/0, 90/10, 80/20 and 60/40 samples on (. . .) cooling and (—) heating measurements. The frequencies used were 1 and 100 kHz.

3.2. Compositional effects

3.2.1. Dielectric properties

Fig. 8a and b show the dielectric permittivity and loss angle tangent as a function of temperature for PMNT100/0, 90/10, 80/20 and 60/40 respectively upon cooling and heating measurements. Decreasing the Ti content, the temperature of spontaneous normal-relaxor transition (T_{nr}) and the permittivity maximum (T_m) are all moved down to low temperature, the spontaneous transition becomes unclear. It is clear that the difference δ between the dielectric permittivity peak temperature and the temperature of the transition from normal ferroelectrics to relaxor ferroelectrics become larger. Otherwise, increasing the Ti content, the relaxor ferroelectric state is absorbed. For PMNT60/40, the δ equals to zero, and the high temperature paraelectric phase directly transforms into low temperature ferroelectric phase.

The PMNT100/0, 90/10 and 60/40 samples were poled by cooling from 250 °C down to lower temperature under a static electric field of 1 kV/ mm. The measurements were then made during heating with the bias field switched off. Fig. 9a and b show the dielectric permittivity and loss angle tangent as a function of temperature for poled samples respectively. The transition temperature of normal-relaxor phase becomes more clear, and does not move with respect to unpoled samples. The strong peaks of the dielectric loss angle tangent are more clear. It confirms the internal strain effect of ferroelectric domain switching.

3.2.2. TEM studies and structure analysis (XRD)

Fig. 10a and b illustrate the room temperature Dark-field images for PMNT90/10 and 60/40 respectively.

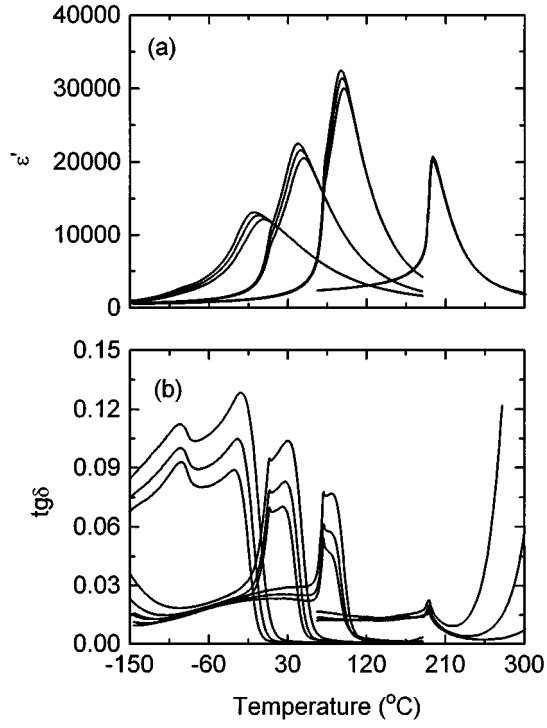

Figure 9 Temperature dependence of the dielectric permittivity (a), and loss angle tangent (b) for poled PMNT100/0, 90/10, 80/20 and 60/40 samples. The frequencies used were 1, 10 and 100 kHz.

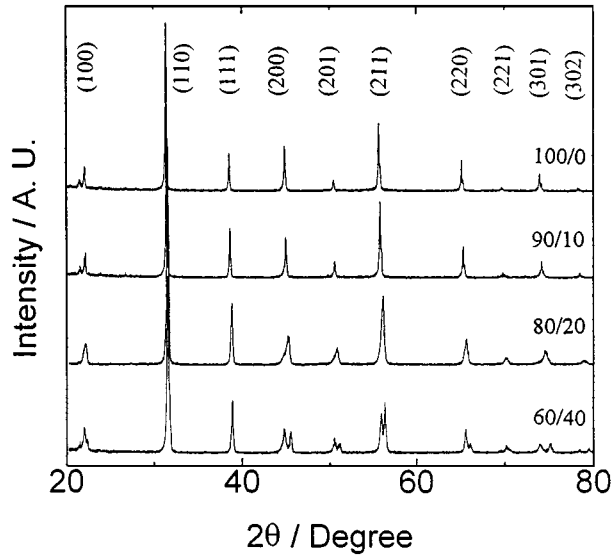

Figure 11 X-ray diffraction patterns of PMNT100/0, 90/10, 80/20 and 60/40 samples.

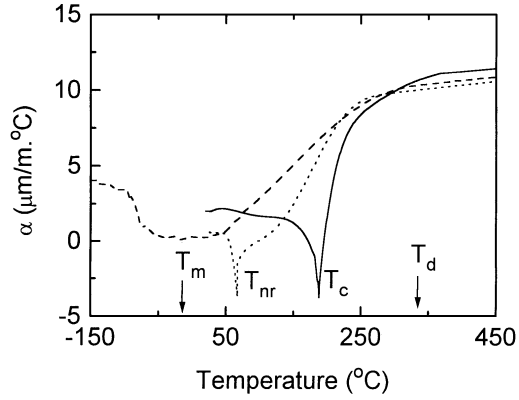

Figure 12 Thermal-expansion coefficient as a function of temperature for (----) PMNT100/0, (....) PMNT80/20 and (—) PMNT60/40 samples.

Various types of domain structures can readily be seen in these micrographs. For PMNT90/10, microdomains are clearly evident. The average size of these microdomains was about 5 nm. With increase of the Ti content, the scale of the polar region/domains increased [19–21]. For PMNT60/40, normal micron-sized ferroelectric macrodomains were clearly found.

From the XRD patterns for PMNT100/0, 90/10, 80/20 and 60/40 respectively shown in Fig. 11, the phase structures are clearly respected to distortion cubic, rhombohedral, and tetragonal phases. It is due to the polar region structure changing.

3.2.3. Thermal expansion measurements

The thermal-expansion coefficient α is shown in Fig. 12 as a function of temperature for PMNT100/0, 80/20 and 60/40 respectively. The transition temperature T_{nr} can be seen clearly from the value of thermal expansion coefficient α minimum. At lower temperatures the slope of thermal expansion was relatively linear for all the samples. However for PMNT 80/20, a distinct lattice

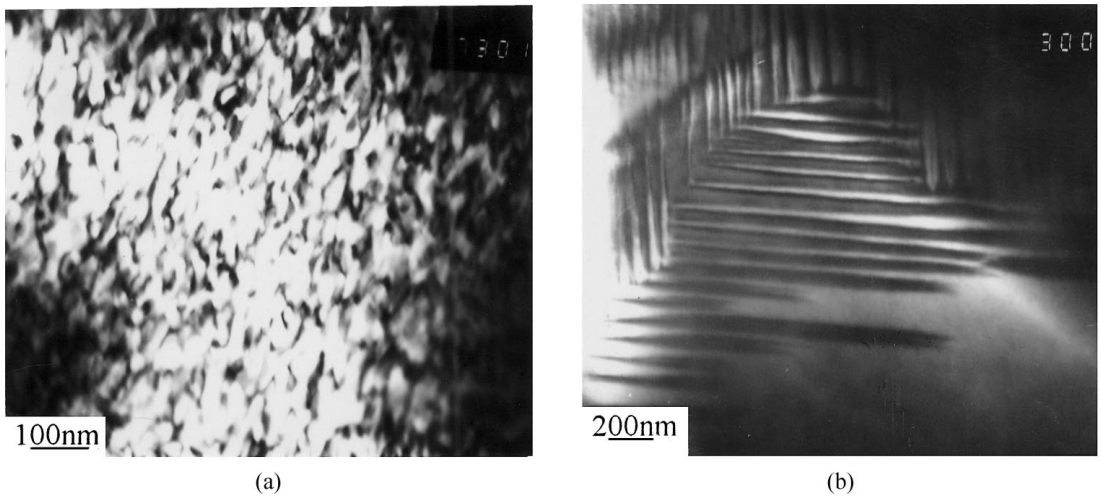

(a) (b)

Figure 10 Dark field TEM images which shown the domain structure for PMNT (a) 90/10, and (b) 60/40 samples respectively.

negative expansion was observed near 68 °C, this expansion, undoubtedly, reflects the normal-relaxor ferroelectric transformation clearly. For PMNT60/40, this transition is absent. For PMNT100/0, the value of thermal-expansion coefficient α minimum did not drop down to zero, but it showed a behavior which can be ascribed wholly by freezing into microdomains of polar microregions, which can be field-induce into long-range ferroelectric state.

4. Conclusions

A first-order relaxor-normal ferroelectric phase transition is clearly observed in $Pb(Mg_{1/3}Nb_{2/3})_{0.8}Ti_{0.2}O_3$ ceramics. Profile analysis of the X-ray diffraction lines show that ⟨111⟩ distorted polar region develop upon cooling. The high dielectric constant values and the permittivity maxima come from the dynamic freezing process of polar region. Microdomains are the frozen polar microregion. The spontaneous, first-order relaxor-normal ferroelectric transition, corresponds to a polar micro-macrodomain switching related to the distorted cubic-rhombohedral phase transition.

Whereas the macroscopic symmetry of relaxor ferroelectric phase is a distorted cubic, at the polar nanodomain level the symmetry is rhombohedral making a spontaneously crossover from displacive to order-disorder type transition possible. It is stressed that the B ions in the oxygen octahedral of $Pb(B'_{1/3}B''_{2/3})O_3$ perovskite relaxors are shifted from center along ⟨111⟩ direction. This is a displacive-type nucleation phase transformation. It is the reason that disordered relaxor state to rhombohedral long-range ordering ferroelectric state. Ferroelectric order-disorder type phase transitions of spontaneous micro-macrodomain switching are likely to be much closer related to structural phase transitions like the stress induced martensitic transitions. The dynamic behavior of polar regions was also affected by the titanium doping.

Acknowledgement

The first author would like to thank Professor W. Ren and Dr. Z. H. Wang for kindly help. This research is supported by the National Natural Science Foundation and Post Doctoral Science Foundation of China.

References

1. G. A. SMOLENSKII, V. A. ISUPOV, A. I. AGRANOVSKAYA and S. N. POPOV, *Sov. Phys. Solid State* **2** (1961) 2584.
2. L. E. CROSS, *Ferroelectrics* **76** (1987) 241.
3. X. YAO, Z. L. CHEN and L. E. CROSS, *J. Appl. Phys.* **54** (1983) 3399.
4. D. VIEHLAND, M. WUTTING and L. E. CROSS, *Ferroelectrics* **120** (1991) 71.
5. S. W. CHOI, T. R. SHROUT, S. J. JANG and A. S. BHALLA, *ibid.* **100** (1989) 29.
6. T. R. SHROUT, Z. P. CHANG, N. KIM and S. MARKGRAF, *Ferroelectrics Lett.* **12** (1990) 63.
7. X. H. DAI and D. VIEHLAND, *J. Appl. Phys.* **74** (1993) 3399.
8. F. CHU, N. SETTER and A. TAGANTSEV, *ibid.* **74** (1993) 5219.
9. M. S. YOON, H. M. JANG and S. KIM, *Jpn. J. Appl. Phys.* **34** (1995) 1916.
10. S. L. SWARTZ and T. R. SHROUT, *Mat. Res. Bull.* **17** (1982) 1245.
11. R. L. BYER and C. B. ROUNDY, *Ferroelectrics* **3** (1972) 333.
12. Y. N. HUANG, Y. N. WANG and H. M. SHEN, *Phys. Rev. B* **46** (1992) 3290.
13. N. A. PERTSEV and G. ARLT, *J. Appl. Phys.* **74** (1993) 4105.
14. G. BURNS, F. H. DACOL, *Phys. Rev. B* **28** (1983) 2527.
15. *Idem.*, *Ferroelectrics* **104** (1990) 25.
16. H. ARNDT and G. SCHMIDT, *ibid.* **79** (1988) 149.
17. G. SCHMIDT, *ibid.* **104** (1990) 205.
18. *Idem.*, *Phase Transitions* **20** (1990) 127.
19. C. RANDALL, A. S. BHALLA, T. R. SHROUT and L. E. CROSS, *J. Mater. Res.* **5** (1990) 829.
20. A. D. HILTON, C. A. RANDALL, D. J. BARBER and T. R. SHROUT, *Ferroelectrics* **93** (1989) 379.
21. J. CHEN, H. M. CHAN and P. M. HARMER, *J. Amer. Ceram. Soc.* **72** (1989) 593.

Received 5 January 1998
and accepted 27 April 1999